Supplement of Atmos. Chem. Phys., 23, 10035–10056, 2023
https://doi.org/10.5194/acp-23-10035-2023-supplement

Atmospheric Chemistry and Physics
Open Access

Supplement of

Constraining the budget of atmospheric carbonyl sulfide using a 3-D chemical transport model

Michael P. Cartwright et al.

Correspondence to: Michael P. Cartwright (mpc24@leicester.ac.uk)

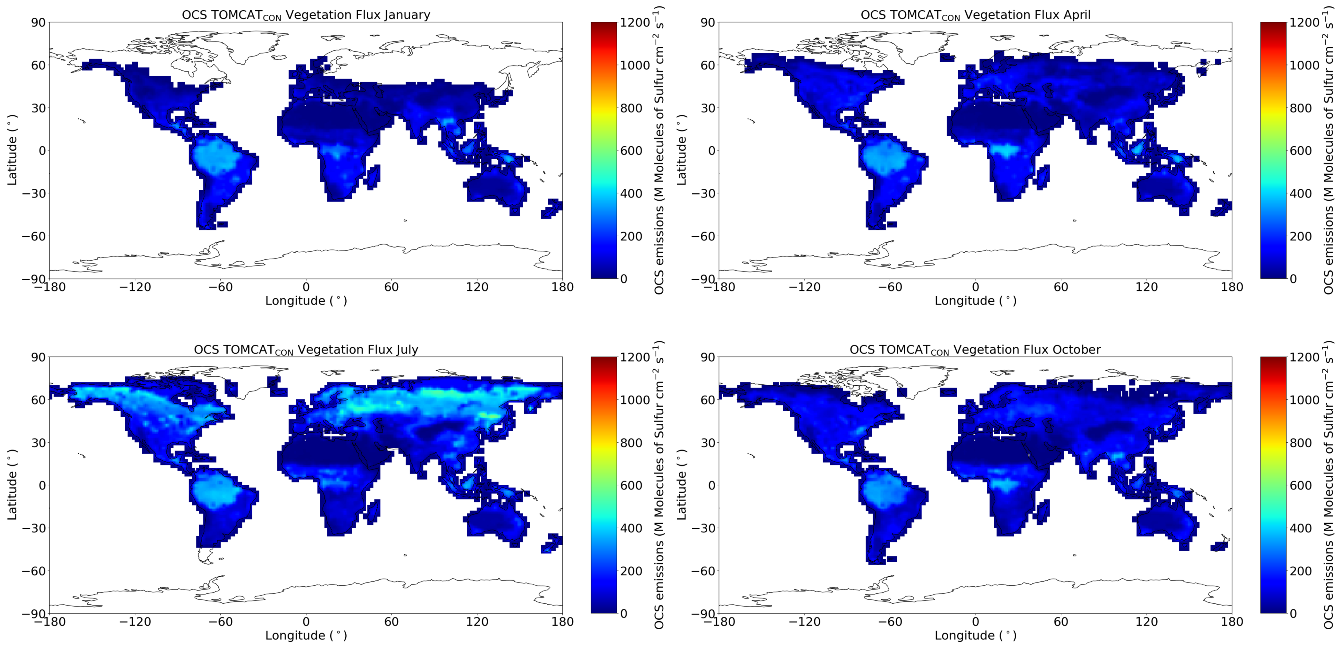

Figure S1. Map of OCS vegetative flux used in the TOMCAT$_{CON}$ simulation for January, April, July, and October of 2010 only (Kettle et al., 2002). The net flux shown is a sink term and in units of M molecules of Sulfur per cm^2 per s.

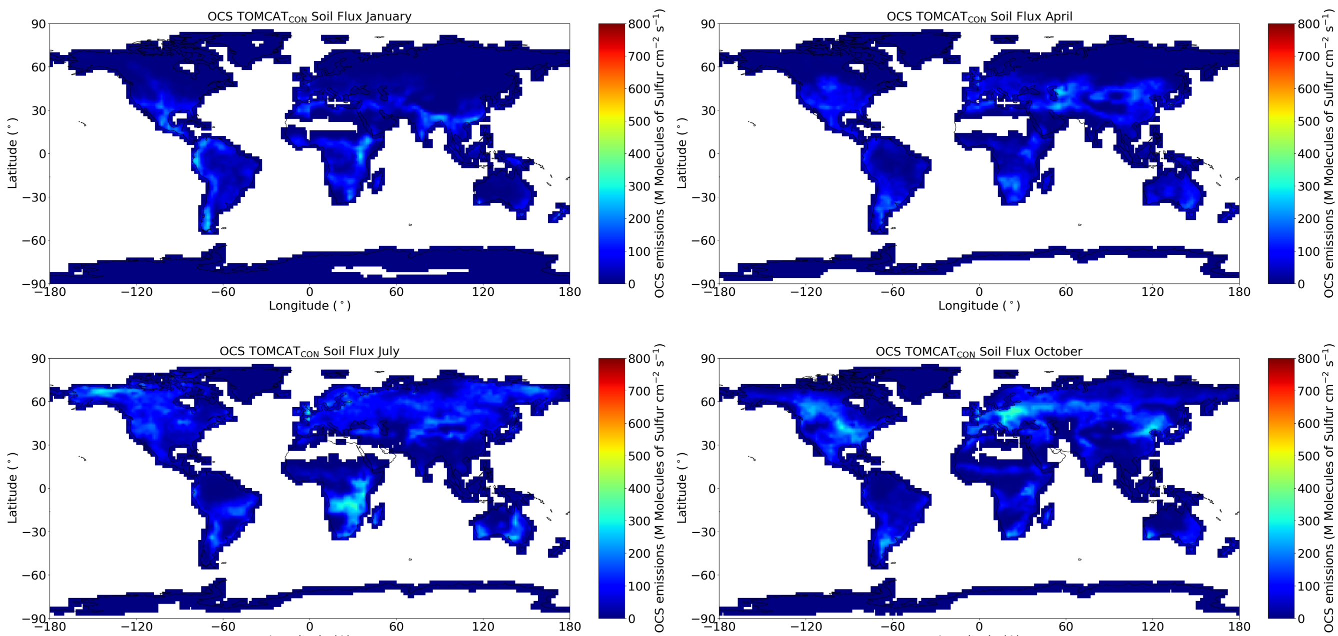

Figure S2. Map of OCS soil flux used in the TOMCAT$_{CON}$ simulation for January, April, July, and October of 2010 only (Kettle et al., 2002). The net flux shown is a sink term and in units of M molecules of Sulfur per cm^2 per s.

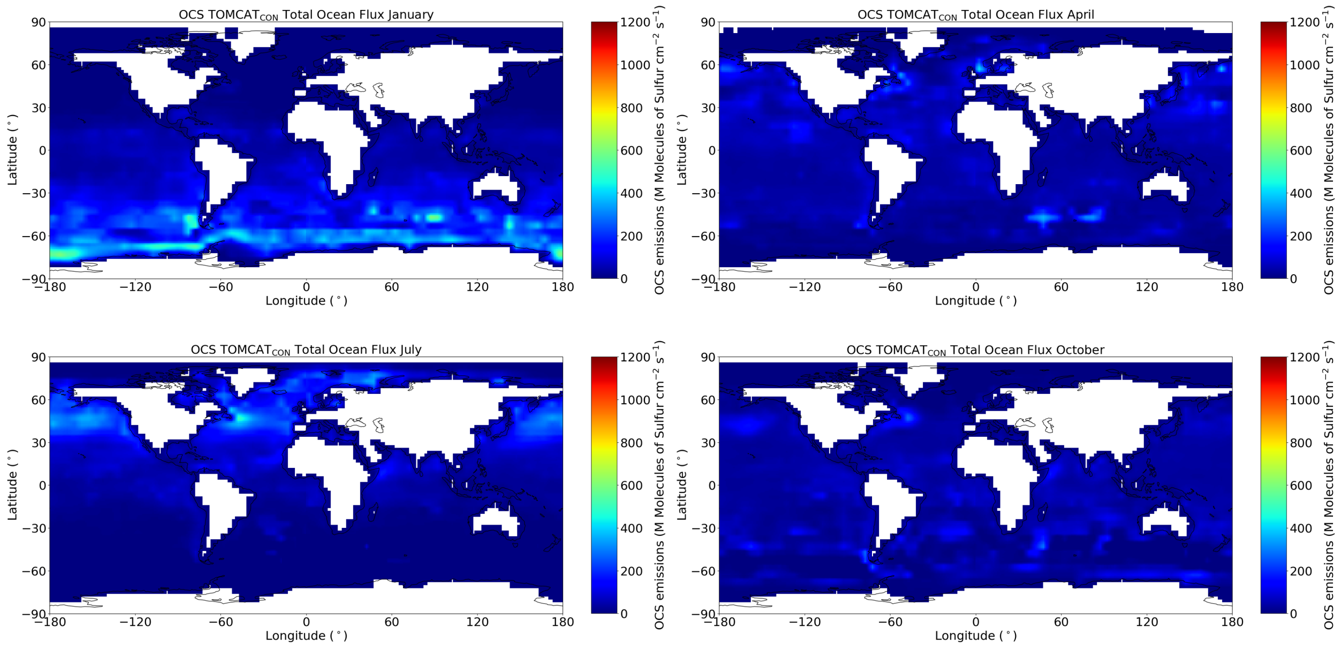

Figure S3. Map of OCS ocean flux used in the TOMCAT$_{CON}$ simulation for January, April, July, and October of 2010 only (Kettle et al., 2002). This represents the combination of all oceanic emission or sink terms. The net flux shown is a source term and in units of M molecules of Sulfur per cm^2 per s. Note a large emission colour bar is used for oceanic emissions to identify hotspots in the emissions used by TOMCAT$_{SOTA}$ and to keep these emissions consistent.

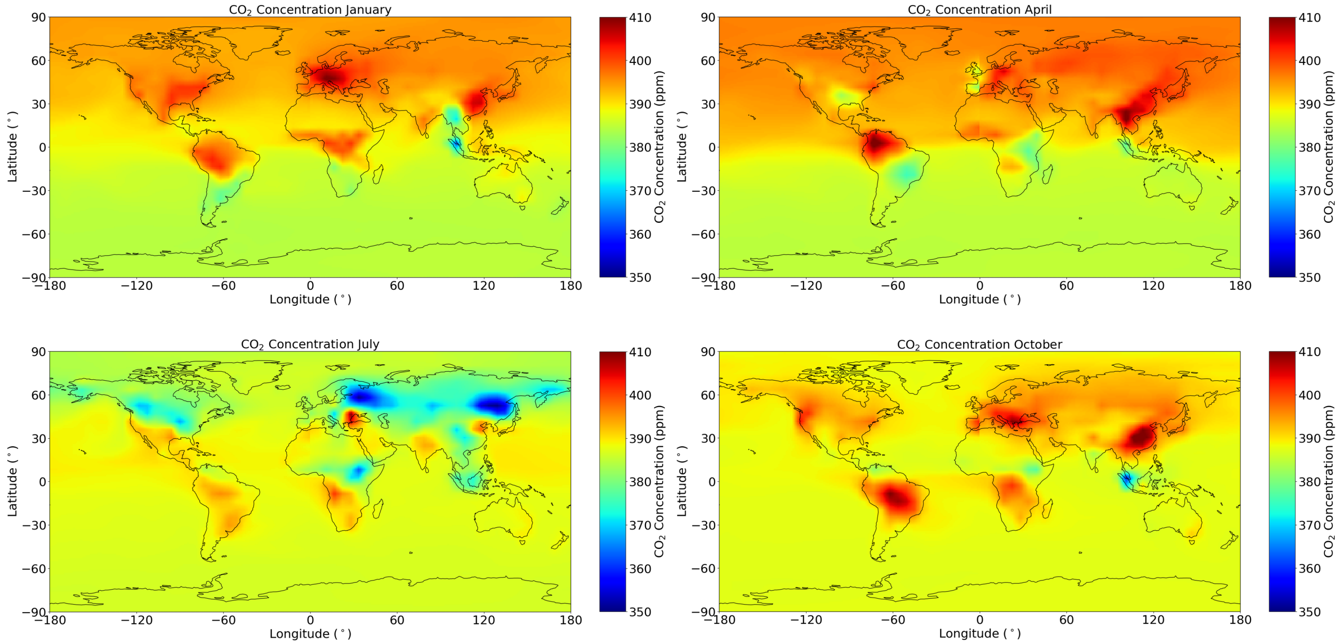

Figure S4. Map of CO_2 concentration (ppm), used in the F_{OCS} calculation shown in Section 3.3.1, for January, April, July, and October of 2010 only.

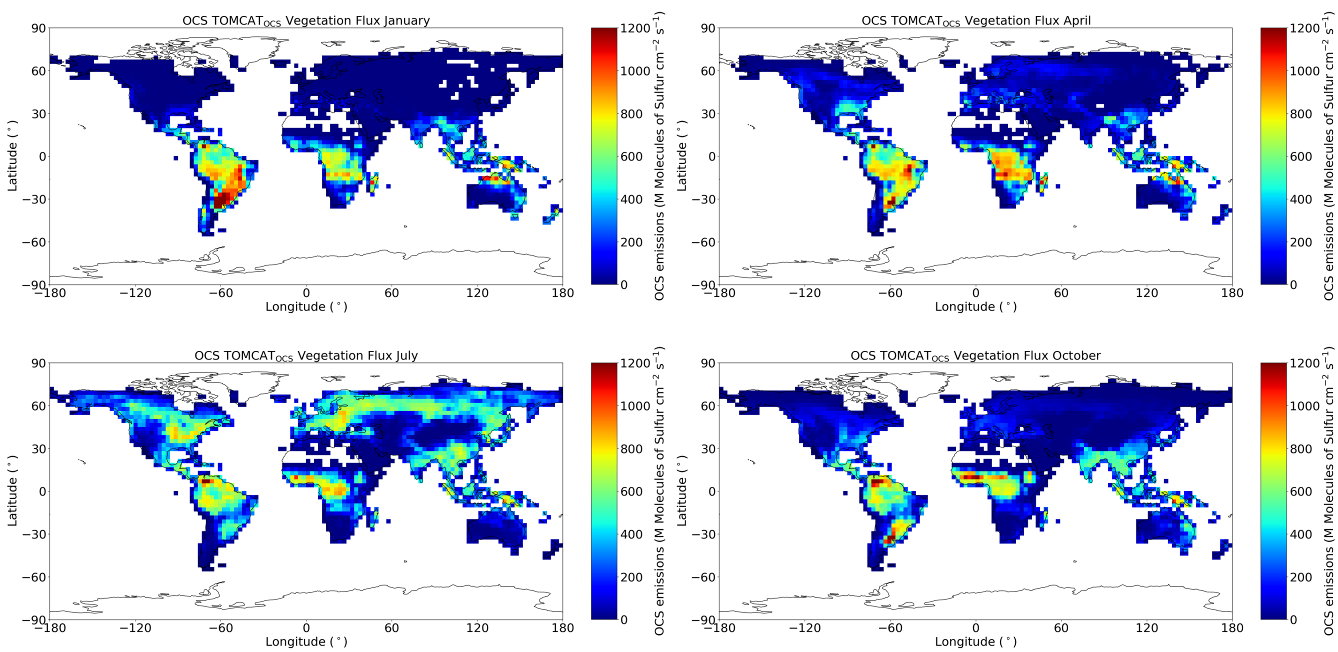

Figure S5. Map of OCS vegetative flux used in the TOMCAT$_{OCS}$ simulation for January, April, July, and October of 2010 only. The net flux shown is a sink term and in units of M molecules of Sulfur per cm^2 per s. Note this flux has the resolution of TOMCAT output, which is a T42 Gaussian grid, approximated to 64x128. This is due to being calculated online within the model.

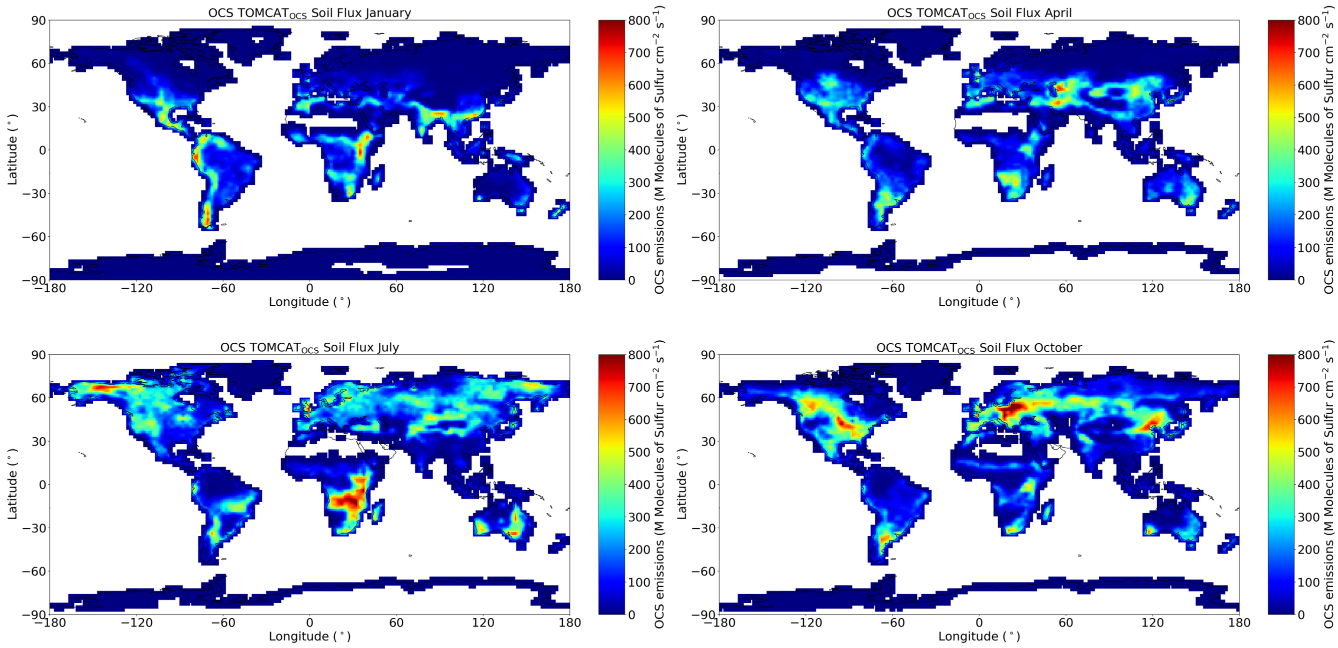

Figure S6. Map of OCS soil flux used in the TOMCAT$_{OCS}$ simulation for January, April, July, and October of 2010 only. The net flux shown is a sink term and in units of M molecules of Sulfur per cm^2 per s.

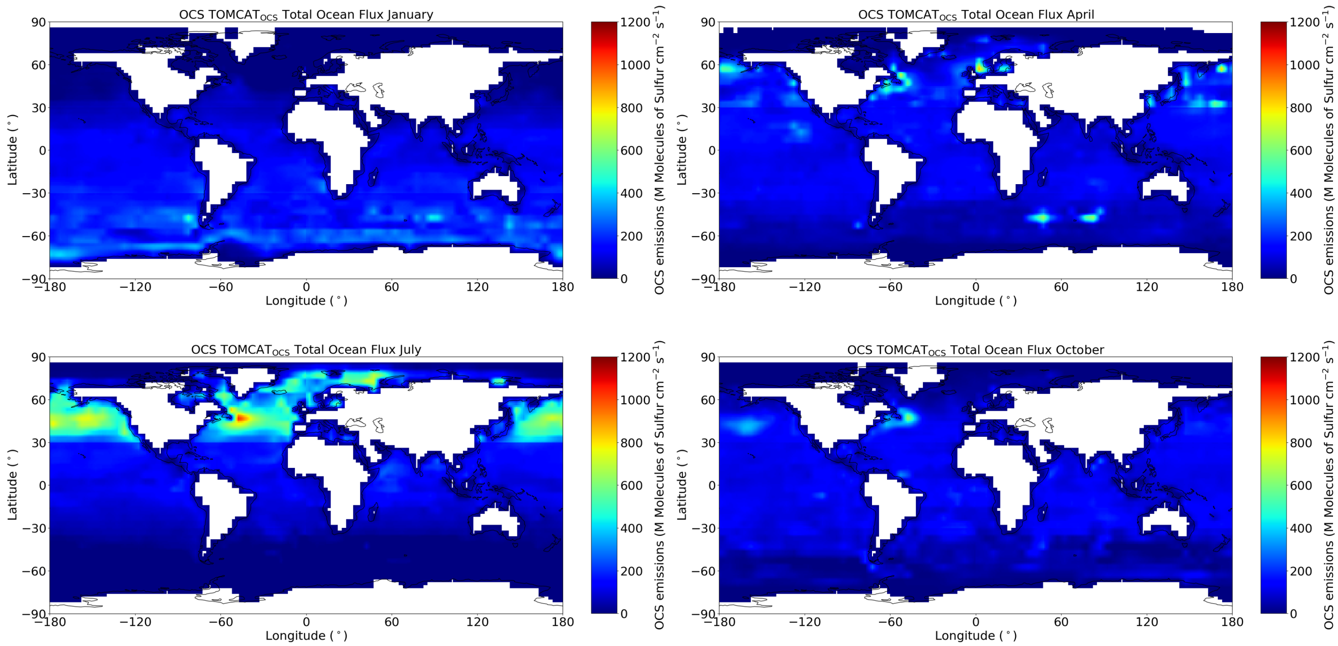

Figure S7. Map of OCS ocean flux used in the TOMCAT$_{OCS}$ simulation for January, April, July, and October of 2010 only (Kettle et al., 2002). This represents the combination of all oceanic emission or sink terms. The net flux shown is a source term and in units of M molecules of Sulfur per cm^2 per s. Note a large emission colour bar is used for oceanic emissions to identify hotspots in the emissions used by TOMCAT$_{SOTA}$ and to keep these emissions consistent.

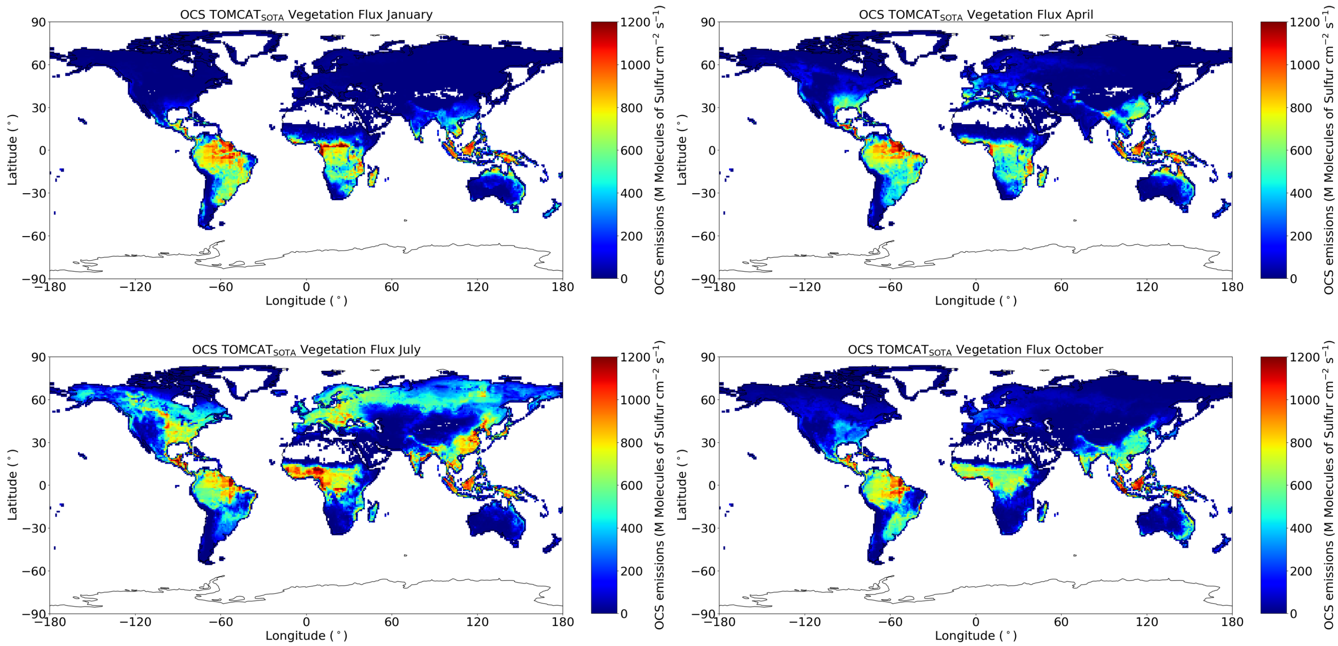

Figure S8. Map of OCS vegetative flux used in the TOMCAT$_{SOTA}$ simulation for January, April, July, and October of 2010 only (Maignan et al., 2021). The net flux shown is a sink term and in units of M molecules of Sulfur per cm^2 per s.

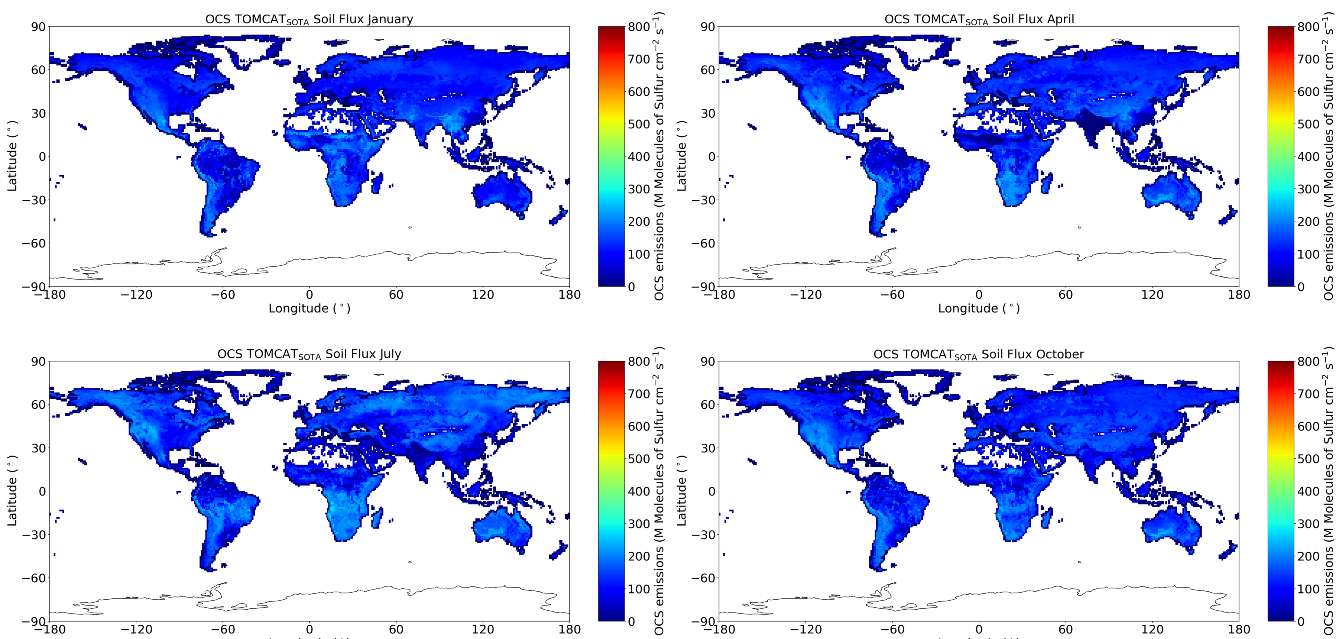

Figure S9. Map of OCS soil flux used in the TOMCAT$_{SOTA}$ simulation for January, April, July, and October of 2010 only. The net flux shown is a sink term and in units of M molecules of Sulfur per cm^2 per s.

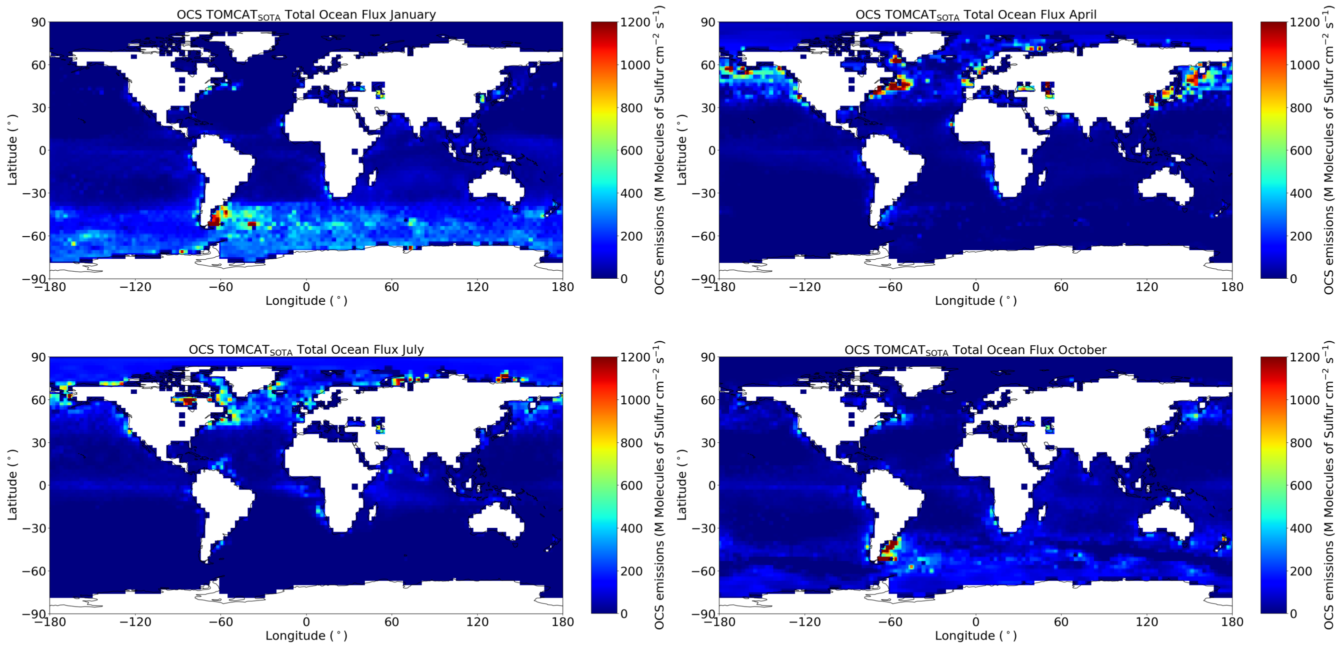

Figure S10. Map of OCS ocean flux used in the TOMCAT$_{SOTA}$ simulation for January, April, July, and October of 2010 only (Lennartz et al., 2017, 2020). The net flux shown is a source term and in units of M molecules of Sulfur per cm^2 per s. Note a large emission colour bar is used for oceanic emissions to identify hotspots in the emissions used by TOMCAT$_{SOTA}$ and to keep these emissions consistent.

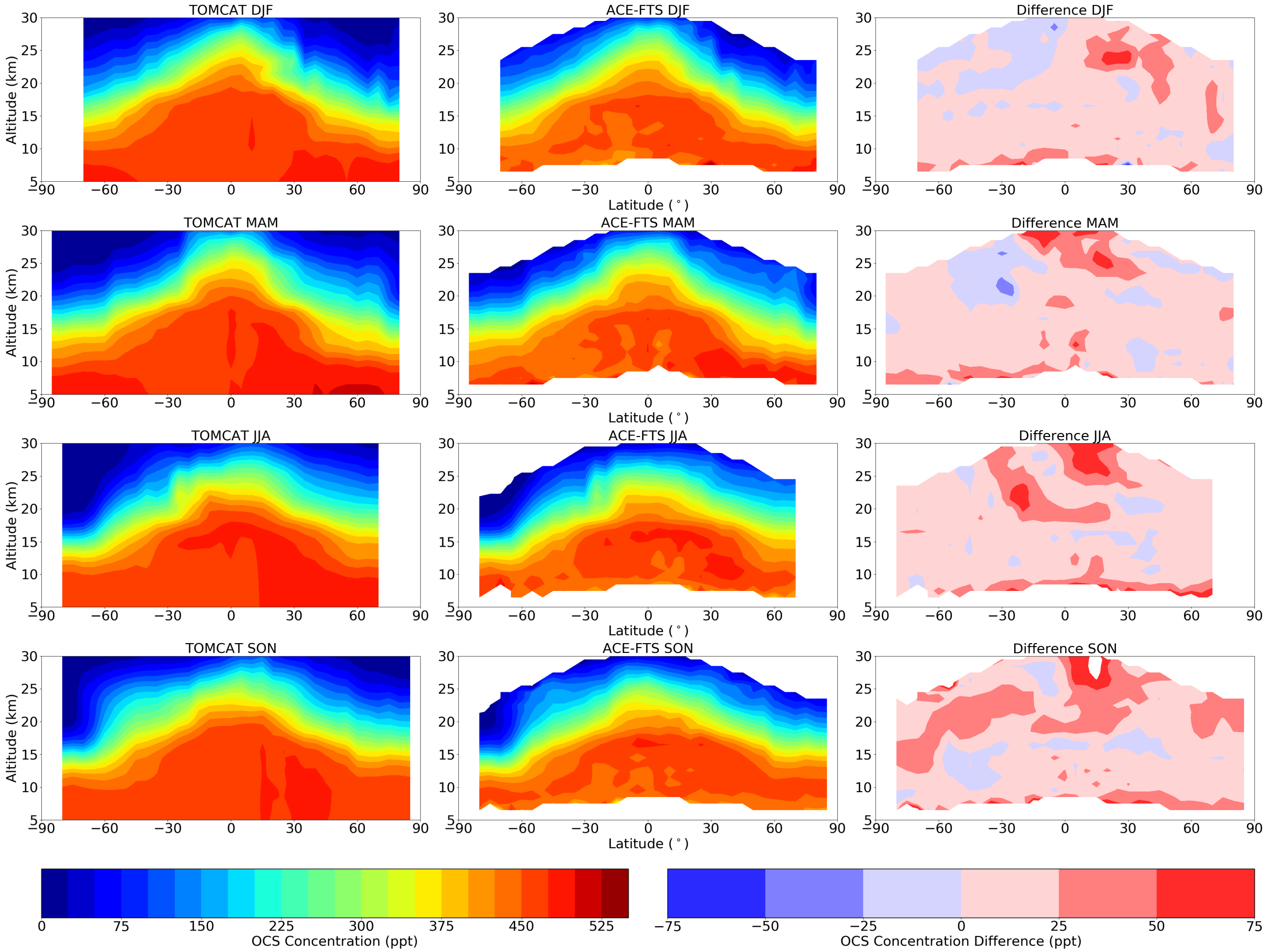

Figure S11. Seasonal zonal mean concentration (mixing ratio) of OCS (ppt) from $TOMCAT_{OCS}$ (left), only for the year 2010 and with a photolysis rate 0.5 times that of $TOMCAT_{OCS}$, ACE (centre) and the difference between the two ($TOMCAT_{OCS}$ minus ACE, right) for the period of 2004 to 2018. $TOMCAT_{OCS}$ and ACE data averaged in 5-degree latitude bins and over all longitudes.

References

Kettle, A. J., Kuhn, U., Hobe, M. von, Kesselmeier, J., and Andreae, M. O.: Global budget of atmospheric carbonyl sulfide: Temporal and spatial variations of the dominant sources and sinks, J. Geophys. Res., 107, ACH 25-1-ACH 25-16, https://doi.org/10.1029/2002JD002187, 2002.

Lennartz, S. T., Marandino, C. A., von Hobe, M., Cortes, P., Quack, B., Simo, R., Booge, D., Pozzer, A., Steinhoff, T., Arevalo-Martinez, D. L., Kloss, C., Bracher, A., Röttgers, R., Atlas, E., and Krüger, K.: Direct oceanic emissions unlikely to account for the missing source of atmospheric carbonyl sulfide, Atmospheric Chemistry and Physics, 17, 385–402, https://doi.org/10.5194/acp-17-385-2017, 2017.

Lennartz, S. T., Marandino, C. A., von Hobe, M., Andreae, M. O., Aranami, K., Atlas, E., Berkelhammer, M., Bingemer, H., Booge, D., Cutter, G., Cortes, P., Kremser, S., Law, C. S., Marriner, A., Simó, R., Quack, B., Uher, G., Xie, H., and Xu, X.: Marine carbonyl sulfide (OCS) and carbon disulfide (CS_2): a compilation of measurements in seawater and the marine boundary layer, Earth System Science Data, 12, 591–609, https://doi.org/10.5194/essd-12-591-2020, 2020.

Maignan, F., Abadie, C., Remaud, M., Kooijmans, L. M. J., Kohonen, K.-M., Commane, R., Wehr, R., Campbell, J. E., Belviso, S., Montzka, S. A., Raoult, N., Seibt, U., Shiga, Y. P., Vuichard, N., Whelan, M. E., and Peylin, P.: Carbonyl sulfide: comparing a mechanistic representation of the vegetation uptake in a land surface model and the leaf relative uptake approach, Biogeosciences, 18, 2917–2955, https://doi.org/10.5194/bg-18-2917-2021, 2021.